Adsorption studies on fruits of Gular (*Ficus glomerata*): Removal of Cr(VI) from synthetic wastewater

Rifaqat A.K. Rao*, Fouzia Rehman

Environmental Research Laboratory, Department of Applied Chemistry, Faculty of Engineering and Technology, Aligarh Muslim University, Aligarh 202002, UP, India

ARTICLE INFO

ABSTRACT

The adsorption of Cr(VI) was studied in batch system using fruits of *Ficus glomerata* as adsorbent. The effect of temperature, pH, initial Cr(VI) concentration and time was investigated. Scanning electron microscopy (SEM) and Fourier transform infrared spectroscopy (FTIR) was used to investigate surface morphology and active functional groups present on the adsorbent surface. Thermodynamic parameters like free energy change (ΔG^0), enthalpy (ΔH^0) and entropy (ΔS^0) indicate the spontaneous, endothermic and increased randomness nature of Cr(VI) adsorption. Equilibrium data were fitted well with Langmuir isotherm at 50 °C. The magnitude of mean free energy indicates chemical nature of adsorption. The breakthrough and exhaustive capacities were found to be 5 and 23.1 mg g^{-1} respectively. The applicability of the adsorbent has been demonstrated by removing Cr(VI) from electroplating wastewater.

1. Introduction

Heavy metals in a water system are hazardous to the environment and humans due to the bio-accumulation through the food chain and persistence in nature. Among all heavy metals, copper chromium and zinc ingestion beyond permissible quantities causes various chronic disorders [1]. Chromium and its compounds are generally released from electroplating, leather tanning, cement, dyeing, fertilizer, photography, paint and pigments, textile, steel fabrication, and canning industries.

Cr(III) and Cr(VI) are two stable oxidation states of chromium that persist in the environment [2]. The trivalent chromium is essential in human nutrition especially in glucose metabolism while most of the hexavalent compounds of chromium are toxic to animals, humans and bacteria and are known to be carcinogenic [3,4]. The maximum concentration limit of hexavalent chromium for discharge into inland surface waters is 0.1 mg L^{-1} and in potable water it is 0.05 mg L^{-1} [5].

Many technologies adopted for the removal of chromium from industrial wastewaters include precipitation, membrane filtration, solvent extraction with amines; ion-exchange, activated carbon adsorption, electro-deposition, and various biological processes [6–11]. Most of these methods suffer set-backs because of high capital and operational cost and lack of skilled personnel problem. Adsorption process has been extensively used for the removal of toxic metals. Recently various low-cost adsorbents such as agriculture wastes and activated carbon prepared from agriculture wastes have been used for the removal of toxic metals from aquatic environment [12–16], where as lichen (*Parmilina tiliaceae*) [17], banana peel [18], tamarind seeds [19], pomegranate husk carbon [20], sunflower (*Helianthus annuus*) stem [21], rice straw [22], *Ficus religiosa* leaf powder [23], spent activated clay [24], have been used for the removal Cr(VI) from water and wastewater.

In present study fruits of *Ficus glomerata* have been used as a new low-cost adsorbent for the removal of Cr(VI) from wastewater. Ficus tree (*F. glomerata*) belongs to Moraceae family. It is 30–50 ft high and found in northern parts of India. This tree has auspicious position and forms a major part of worship religious festivals. The Ficus fruit is 2 in. in diameter. Fruits are green in colour when unripe and are found in groups. The fruition period is from March to June. The tree has various applications in Ayurveda medicines as astringent, antidiuretic and leucorrhea and menstrual disorders. Fruit of Ficus are used to treat anemia and gastrointestinal disorders [25]. The effect of various parameters such as pH, contact time, adsorbent amount and initial Cr(VI) concentration were studied and discussed in detail in the following sections.

2. Materials and methods

2.1. Adsorbent

Fruits of Ficus were collected locally and dried, crushed and washed several times with double distilled water till the water was clear of all coloration and finally dried in an air oven at

* Corresponding author. Tel.: +91 0571 2703167x3000.
E-mail address: rakrao1@rediffmail.com (R.A.K. Rao).

100–105 °C for 24 h. After drying the adsorbent was sieved through 150–300 μm size and used as such.

2.2. Adsorbate solution

Stock solution of Cr(VI) was prepared (1000 mg L^{-1}) by dissolving the desired quantity of potassium dichromate (AR grade) in double distilled water (DDW).

2.3. Determination of point of zero charge (pH$_{PZC}$)

The zero surface charge characteristics of the *F. glomerata* fruits were determined by using the solid addition method [26]. 40 mL of 0.1 M KNO$_3$ solution was transferred to a series of 100 mL conical flasks. The initial pH (pH$_0$) of the solutions was roughly adjusted between 2 and 8 by adding either 0.1 M HCl or 0.1 M NaOH. The total volume of the solution in each flask was adjusted exactly to 50 mL by adding KNO$_3$ of the same strength. Initial pH (pH$_0$) of the solutions was then accurately noted with the help of pH meter. 0.5 g of adsorbent was then added to each flask and allowed to equilibrate for 24 h with intermittent manual shaking. The final pH (pH$_f$) of the supernatant liquid was noted. The difference between the initial pH (pH$_0$) and final pH (pH$_f$) values (ΔpH = pH$_0$ − pH$_f$) were plotted against pH$_0$. The point of intersection of the resulting curve with abscissa, at which ΔpH 0, gave the pH$_{PZC}$. The same procedure was repeated using 0.001 M and 0.01 M KNO$_3$ solutions.

2.4. Adsorption studies

Adsorption studies were carried out by batch process. 0.5 g adsorbent was placed in a conical flask, 50 mL solution of metal ions of desired concentration was added and the mixture was shaken in shaker incubator for 24 h. The mixture was then filtered by Whatman filter paper No. 41 and final concentration of metal ions was determined in the filtrate by atomic absorption spectrometry (AAS) (Model GBC 902, Australia). The amount of metal ions adsorbed was calculated by subtracting the final concentration from initial concentration [27].

2.5. Effect of pH

The effect of pH on the adsorption of Cr(VI) was studied as follows. 100 mL of Cr(VI) solution was taken in a series of beakers. The desired pH of solution was adjusted in each beaker by adding 0.1 M HCl or NaOH solution. The concentration of Cr(VI) in this solution was then determined (initial concentration). 50 mL of this solution was taken in a series of conical flasks and treated with 0.5 g of adsorbent for 24 h in shaker incubator. The mixture was then filtered and final concentration of Cr(VI) in filtrate was determined as described above. To study the effect of ionic strength Cr(VI) solution (50 mg L^{-1}) was prepared in 0.01 and 0.1 M KNO$_3$ solutions. The pH of these solutions was adjusted in between 2 and 9 as described above.

2.6. Effect of time

A series of 250 mL conical flasks, each having 0.5 g adsorbent and 50 mL solution of known Cr(VI) concentration (10, 20, 40, 50, 80 and 100 mg L^{-1}) were shaken in a shaker incubator and at the predetermined intervals, the solution of the specified flask was taken out and filtered. The concentration of Cr(VI) in the filtrate was determined by AAS and the amount of Cr(VI) adsorbed in each case was then determined as described above.

2.7. Effect of adsorbent dose

A series of 250 mL conical flasks, each containing 50 mL of Cr(VI) solution of 50 mg L^{-1} concentration were treated at 30 °C with varying amount of adsorbent (0.1–1.0 g). The conical flasks were shaken in a shaker incubator for 24 h. The solutions were then filtered and amount of Cr(VI) adsorbed in each case was calculated as described above. The same procedure was repeated at 40 and 50 °C.

2.8. Breakthrough capacity

0.5 g of adsorbent was taken in a glass column (0.6 cm internal diameter) with glass wool support. 1 L of Cr(VI) solution with 50 mg L^{-1} initial concentration (C_0) was prepared. The pH of this solution was adjusted to 2 and then passed through the column with a flow rate of 1 mL min^{-1}. The effluent was collected in 50 mL fractions and the amount of Cr(VI) was determined in each fraction (C) with the help of AAS. The breakthrough curve was obtained by plotting C/C_0 versus volume of the effluent.

2.9. Desorption of Cr(VI) by batch process

Attempts were made to desorb Cr(VI) by batch process. 0.5 g adsorbent was treated with 50 mL of Cr(VI) solution (50 mg L^{-1}). The adsorbent was washed several times with distilled water to remove excess of Cr(VI) ions. Adsorbent was then treated with 50 mL 0.1 M NaOH solution and after 24 h the amount of Cr(VI) desorbed was determined. The experiment was repeated several times to check the reproducibility.

2.10. Analysis of electroplating wastewater

Electroplating wastewater was collected from one of the lock factory in Aligarh city. The pH of the wastewater was 5.6 at the time of sample collection. Analysis of heavy metals ions in electroplating wastewater was carried out by AAS. Total dissolved salts (TDS) were determined by evaporating 100 mL wastewater in a china dish.

2.11. Treatment of electroplating wastewater by batch process

50 mL wastewater of initial pH 5.6 was taken in a conical flask and then its pH was adjusted to 2 and then 0.5 g adsorbent was added. The mixture was shaken and then kept for 24 h. It was filtered and filtrate was analyzed for heavy metals by AAS.

2.12. Treatment of electroplating wastewater by column process

In another experiment, 50 mL electroplating wastewater was taken in a beaker and its pH was adjusted to 2. It was passed through the column containing 0.5 g adsorbent, with a flow rate of 1 mL min^{-1}. The effluent was collected in a beaker and then analyzed for heavy metals by ASS.

3. Results and discussion

3.1. Characterization of adsorbent

Scanning electron microscopy (SEM) observations (Fig. 1a and b) showed rough surface of the adsorbent that provides large surface area for adsorption. However, adsorbent showed no change in its morphology after Cr(VI) adsorption.

FTIR spectra of Ficus before and after Cr(VI) adsorptions are shown in Fig. 2a and b respectively. The band at 2926 cm^{-1} is due to C–H vibrations of aliphatic acid [28]. The two peaks at 1426 and 1630 cm^{-1} indicate the presence of COO and C=O groups. A significant shift of these peaks from 1630 to 1514 cm^{-1} and 1426 to
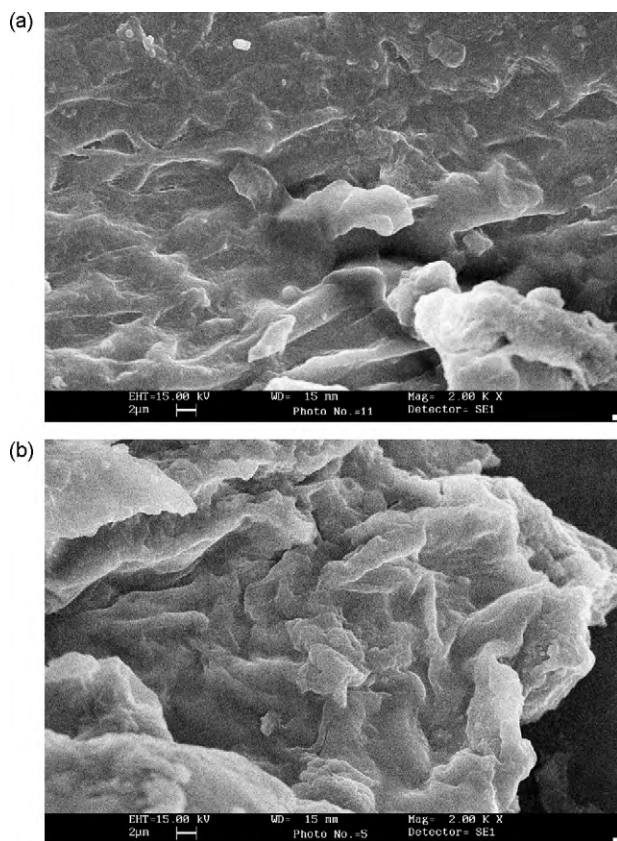
Fig. 1. (a) SEM image of native adsorbent and (b) SEM image of adsorbent after Cr(VI) adsorption.
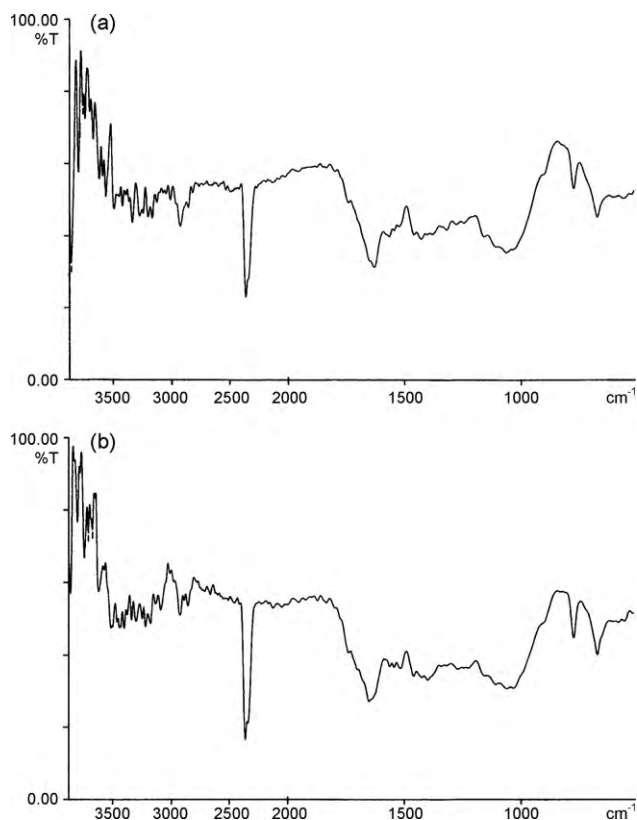

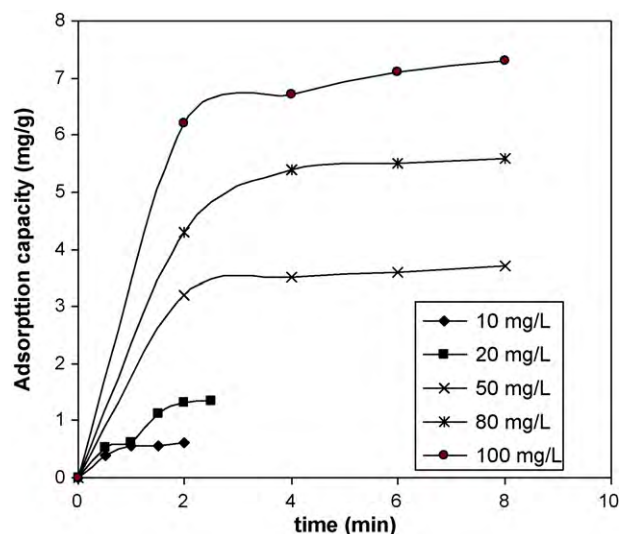**Fig. 2.** (a) FTIR of native adsorbent and (b) FTIR of adsorbent after Cr(VI) adsorption.

Fig. 3. Effect of contact time and initial concentration.

1398 cm^{-1} occurs perhaps due to the fact that carboxylic groups are protonated on unionized at pH 2 and make surface positively charged which is responsible for the adsorption of Cr(VI) at pH 2 The band at 1060 cm^{-1} is due to stretching vibration of C–OH group of carboxylic acid [28]. The band at 1060 cm^{-1} is also shifted to 1058 cm^{-1} after Cr(VI) adsorption.

### 3.2. Effect of initial concentration, contact time and doses

The effect of contact time on the adsorption of Cr(VI) at different initial concentrations (10–100 mg L^{-1}) is represented in Fig. 3. These data were recorded at constant pH (pH 2). Adsorption increases rapidly at initial stage and then gradually reaches towards equilibrium. The contact time needed for Cr(VI) solutions with initial concentrations of 10 and 20 mg L^{-1} to reach equilibrium was found to be 1 and 2 min while solutions with initial Cr(VI) concentrations of 50, 80 and 100 mg L^{-1} needed 4 min to attain equilibrium. This is due to the fact that Cr(VI) ions are adsorbed more quickly onto the surface at lower concentration but at higher initial concentration, Cr(VI) ions diffuse into the inner sites of the adsorbent which is a slow step. The amount of Cr(VI) adsorbed at equilibrium increases with increase in initial concentration. This is because of the increase in concentration gradient and driving force with increased concentration. The adsorption capacity of Cr(VI) at equilibrium was found to be 0.63, 1.31, 3.5, 5.4 and 6.7 mg g^{-1} respectively at initial concentrations of 10, 20, 50, 80 and 100 mg L^{-1}. The effect of adsorbent dose (0.2–1.0 g) indicates increase in percentage adsorption from 74 to 98% and decrease in adsorption density from 10 to 2.45 mg g^{-1} at pH 2 which may be attributed to increased surface area of the adsorbent and availability of more adsorption sites due to increased amount of adsorbent.

3.3. Effect of pH

The adsorption of Cr(IV) from 50 mg L^{-1} chromium solution at various controlled pH values are represented in Fig. 4. Adsorption increases from 10 to 96% when pH decreased from 10 to 2. The increase in Cr(VI) removal with decrease in solution pH was also observed on peat [30], fungal biomass [31] and bacterium biomass [32]. At optimal acidic condition (pH 2), the dominant species of Cr(VI) ions in solution are HCrO$_4$$^-$, Cr$_2O_7$$^{2-}$, Cr$_3O_{10}$$^{2-}$ and Cr$_4$O$_{13}$$^{2-}$ [33]. These anionic species could adsorb on protonated active sites of the adsorbent, though at highly acidic pH (pH 1), Cr(VI) anions are

Table 1
Langmuir and Freundlich isotherms parameters for the adsorption of Cr(VI).

Temperature (°C)	qm (mg g^{-1})	b (L mg^{-1})	r^2	χ^2	RL	K_f	$1/n$	r^2	χ^2
30	31.6	0.0145	0.998	3.490	0.5797	0.0388	2.097	0.999	2.07
40	14.43	0.0502	0.9914	0.652	0.2849	1.0900	0.631	0.9991	4.30
50	46.73	0.0236	0.9998	0.168	0.4587	1.0400	0.959	0.9951	0.95
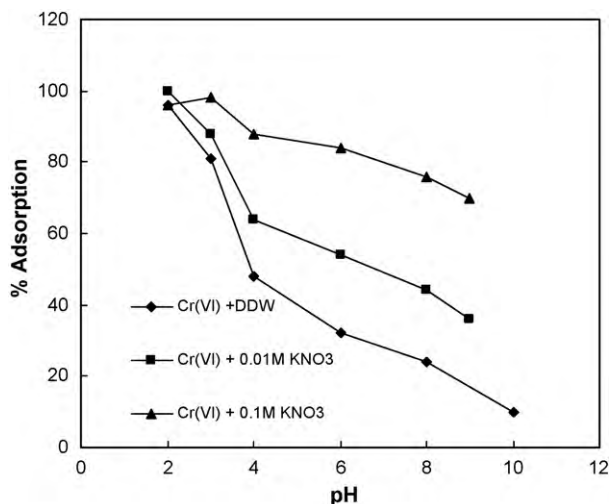
Fig. 4. Effect of electrolyte concentration on the adsorption of Cr(VI) at different pHs.

likely to get reduced to Cr(III) ions which due to electrostatic repulsive forces, are poorly adsorbed [34]. At very low pH values, the surface of the adsorbent is surrounded by hydronium ions which enhance the Cr(VI) interaction with binding sites of adsorbent by greater attractive forces [35]. Then, as the pH increases, there is a gradual reduction in the degree of protonation and therefore, % adsorption decreases [36]. Adsorption of Cr(VI) at different pHs in presence KNO$_3$ (to maintain ionic strength) indicates that adsorption of Cr(VI) at pH 2 is not effected in presence of appreciable amount of KNO$_3$ (Fig. 4). The adsorption of Cr(VI) in aqueous solution, 0.01 M KNO$_3$ and 0.1 M KNO$_3$ is almost constant (96, 100 and 100% respectively) at pH 2. Fig. 5 shows effect of electrolyte concentration on the surface charge of the adsorbent. The pH$_{PZC}$ is shifted
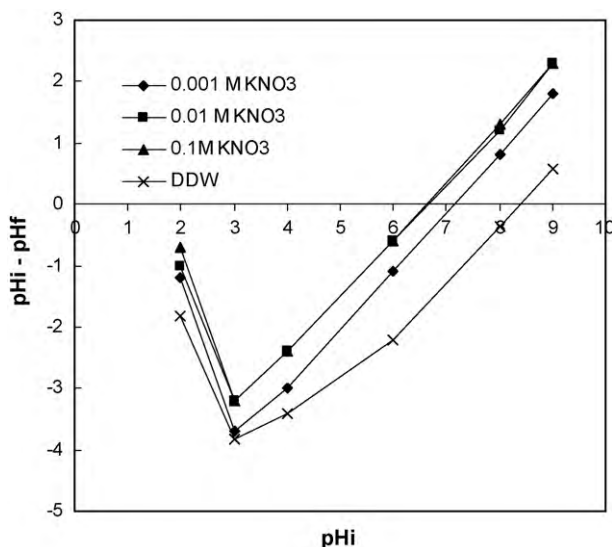
Fig. 5. Point of zero charge.

towards lower pH with increase in electrolyte concentration showing specific adsorption of counter ions [37]. The pH$_{PZC}$ in DDW is 8.2 and shifted to 6.8 at higher concentration of electrolyte (KNO$_3$). It can be inferred from Fig. 5 that in neutral solution the surface charge of the adsorbent is negative at pH < 8.2, neutral at pH 8.2 and positive at pH > 8.2 but in presence of 0.01 and 0.1 M KNO$_3$, the surface charge has shifted to 6.8 and hence appreciable amount of Cr(VI) has been adsorbed (84%) in presence of 0.1 M KNO$_3$ at pH $\leq$ 6 (Fig. 4).

3.4. Adsorption isotherms

The adsorption isotherm data were analyzed using Langmuir and Freundlich isotherm equations [38].

The linear form of Langmuir isotherm is represented as

$$\frac{1}{qe} = \frac{1}{qm} \times \frac{1}{b} \times \frac{1}{Ce} + \frac{1}{qm} \tag{1}$$

where qe is the amount of metal adsorbed per unit weight of adsorbent, qm is the maximum sorption capacity (mg g^{-1}) determined by the number of reactive surface sites in an ideal monolayer system, Ce is the concentration of metal ions at equilibrium (mg L^{-1}) and b is related to bonding energy associated with pH dependent equilibrium constant. Plots of $1/qe$ versus $1/Ce$ at 30, 40 and 50 °C give straight lines (figure not shown) and values of b and qm were calculated from the slope and intercept of the plots. The values of b and qm at different temperatures are reported in Table 1. A chi-square (χ^2) test was also applied to this model. The advantage of χ^2 test is that qe (cal) from the model and qe determined experimentally (qe(exp)) can be compared on the same abscissa and ordinate [39]. If data from model were similar to the experimental data, χ^2 would be small and vice versa. Values of χ^2 were calculated using the following relation.

$$\chi^2 = \sum \frac{(qe(\exp) - qe(\text{cal}))^2}{qe(\text{cal})} \tag{2}$$

The value of χ^2 is least at 50 °C (Table 1) and also the regression coefficient (r^2) is high (0.9998) showing that Langmuir isotherm is best fitted at 50 °C.

The linear form of Freundlich isotherm can be represented as

$$\log qe = \log K_f + \frac{1}{n} \log Ce \tag{3}$$

where K_f is Freundlich constant and n is another constant that informs about the heterogeneity degree of the surface sites. When n approaches zero, the surface heterogeneity increases. Plots of $\log qe$ versus $\log Ce$ give straight lines at 30,40 and 50 °C (figure not shown) and values of n and K_f were calculated from the slope and intercept of these plots (Table 1). The values of χ^2 at different temperatures are also shown in Table 1. The least value of χ^2 and high correlation coefficient (r^2) (0.9951) at 50 °C indicates that Freundlich isotherm is also obeyed at 50 °C. When Langmuir and Freundlich isotherms are compared at 50 °C, the χ^2 value for Langmuir isotherm is lower (0.168) than that obtained from Freundlich isotherm (0.951) hence it can be concluded that both Langmuir and Freundlich models are obeyed by the system at 50 °C but Langmuir model is a better fit.

The essential characteristic of Langmuir isotherm can be expressed in terms of dimensionless constant separation factor or

equilibrium parameter RL, given by the following relation:

$$RL = 1/1 + b \times C_0 \tag{4}$$

where b is the Langmuir constant and C_0 is the initial concentration of Cr(VI) (mg L^{-1}). RL value predicts the shape of the isotherm. If RL > 1 unfavorable, RL = 1 linear, 0 < RL < 1 favorable and RL = 0 for irreversible adsorption [40]. The RL values at 30, 40 and 50 °C are shown in Table 1. The values of RL in the range 0–1 at all these temperatures show favorable adsorption of Cr(VI).

The Dubinin and Radushkevich isotherm [41] is based on the heterogeneous nature of the adsorbent surface, was used to predict the physical or chemical nature of the adsorption process. The D–R equation may be given as

$$\ln qe = \ln qm - \beta \varepsilon^2 \tag{5}$$

where qe is the adsorption capacity (mol g^{-1}) and qm is the maximum adsorption capacity (mol g^{-1}), β is the activity coefficient constant and ε is the polyanyi potential which is given as

$$\varepsilon = RT \ln \left(1 + \frac{1}{Ce}\right) \tag{6}$$

where R is the gas constant (kJ mol^{-1}) and T is the temperature in Kelvin. Ce is the equilibrium concentration (mol L^{-1}). The values of qm and β can be obtained from the intercept and slope of the linear plot of ln qe versus ε^2 at different temperatures (figure not shown). The mean free energy of adsorption E can be calculated from the following equation:

$$E = \frac{1}{\sqrt{-2\beta}} \tag{7}$$

The D–R parameters and mean free energy along with correlation coefficients (r^2) are given in Table 2. The values of E obtained which are in the energy range of chemical adsorption [42].

3.5. Thermodynamic studies

The temperature range used in this study was 30–50 °C. The equilibrium constants (Kc) at 30, 40 and 50 °C were calculated from the following relation [43].

$$Kc = \frac{C_{AC}}{Ce} \tag{8}$$

where C_{AC} and Ce are the equilibrium concentrations (mg L^{-1}) of Cr(IV) on the adsorbent and in solution, respectively. Free energy change (ΔG^0) can be calculated as

$$\Delta G^0 = -RT \ln Kc \tag{9}$$

where T is the absolute temperature and R is gas constant. The value of enthalpy change (ΔH^0) and entropy change (ΔS^0) were calculated from the following relation:

$$\ln Kc = \Delta S^0/R - \Delta H^0/R \times 1/T \tag{10}$$

ΔS^0 and ΔH^0 were calculated from the slope and intercept of linear plot of ln Kc versus $1/T$ (figure not shown). The values of Kc, ΔH^0, ΔS^0 and ΔG^0 are reported in Table 3. The positive value of ΔH^0 indicates endothermic process. The decrease in ΔG^0 with increase in temperature indicates that the process is spontaneous and spontaneity increases with increase in temperature. The positive value of ΔS^0 suggests increase randomness at the solid–liquid interface during adsorption.

3.6. Adsorption kinetics

The rate constants for the adsorption of Cr(VI) were calculated by using pseudo-first-order and pseudo-second-order equations.
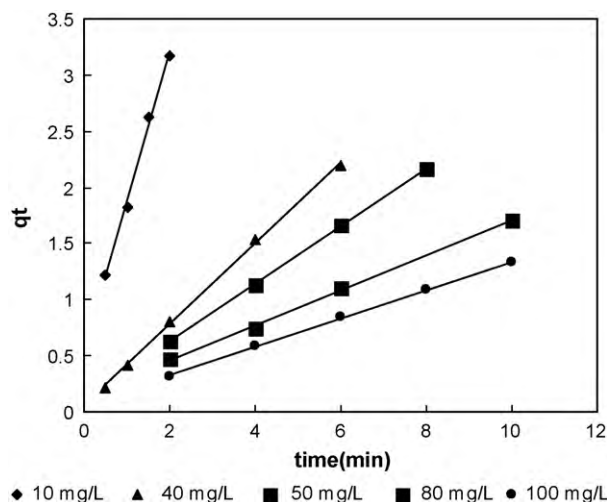

Fig. 6. Pseudo-second-order kinetics.

The pseudo-first-order [44] and pseudo-second-order [45] equations are based on solution concentration. The pseudo-first-order expression is given by equation.

$$\log(qe - qt) = \log qe - K_1 \times 1/2.303 \times t \tag{11}$$

where qe is the adsorption capacity (mg g^{-1}) at equilibrium, qt is the adsorption capacity at time (t) and K_1 (min^{-1}) is the pseudo-first-order adsorption rate constant. Linear plots of $\log(qe-qt)$ versus t were observed at different initial Cr(VI) concentrations (figure not shown). The regression coefficients (r^2) and rate constants at various concentrations are reported in Table 4. The pseudo-second-order adsorption kinetics rate equation [46] is given as

$$1/qt = 1/h + 1/qe \times t/1 \tag{12}$$

where h is the initial adsorption rate (mg g^{-1} min^{-1}), which is given as $h = K_2 \times qe^2$.

K_2 (g mg^{-1} min^{-1}) is the rate constant for pseudo-second-order reaction. The values of K_2 were calculated from the slope of the linear plots of t/qt versus t (Fig. 6). These values are reported in Table 4. A comparison of the experimental adsorption capacities (qe(exp)) and calculated values (qe(cal)) obtained from Eqs. (11) and (12) show that pseudo-second order model obeyed better than pseudo-second order.

3.7. Intra-particle diffusion

The Weber and Morris [47] intra-particle diffusion model can be expressed as

$$qt = Kid \times t^{1/2} + I \tag{13}$$

where qt (mg g^{-1}) is the amount of Cr(VI) adsorbed at time t, I (mg g^{-1}) is the intercept and Kid (mg g^{-1} min$^{-1/2}$) is the intra-particle diffusion rate constant. The Kid values obtained from the slope of the curve of different initial Cr(VI) concentrations (Fig. 7) are shown in Table 5. The r^2 values (between 0.8842 and 0.9894) suggest that adsorption of Cr(VI) can be followed by intra-particle diffusion model. However, plots did not pass through the origin (the intercept values are between 0.20 and 5.1 mg g^{-1}) indicating that intra-particle diffusion is not the only rate-limiting step. The increase in intercept values with increase in concentration is indicative of increased boundary layer effect [29].

Table 2
Dubinin–Radushkevisk (D–R) parameters for the adsorption of Cr(VI) at pH 2.

Temperature (°C)	β (mol k^{-2} J^{-2})	$\ln qm$	qm (mol g^{-1}) × 10^{-5}	Ea (KJ mol^{-1})	r^2
30	−0.0130	−06.97	93.80	6.2	0.9980
40	−0.0061	−10.25	03.50	9.1	0.9953
50	−0.0062	−09.38	8.37	9.0	1.0000

Table 3
Thermodynamics parameters at different temperatures for the adsorption of Cr(VI) at pH 2.

Temperature (°C)	Kc	ΔG^0 (kJ mol^{-1})	ΔH^0 (kJ mol^{-1})	ΔS^0 (kJ mol^{-1} K^{-1})	r^2
30	8.60	−5.40	62.74	0.239	0.9978
40	11.82	−6.43			
50	20.70	−8.14			

Table 4
Pseudo-first-order and pseudo-second-order rate parameters for the adsorption of Cr(VI) at different concentrations (pH 2).

Concentration (Co) (mg L^{-1})	Pseudo-first-order				Pseudo-second-order			
	qe (experimental)	qe (calculated) (mg g^{-1})	K_1	r^2	qe (calculated) (mg g^{-1})	K_2	h	r^2
10	0.72	0.640	1.37	0.999	0.75	0.93	1.83	0.9944
40	2.70	0.476	0.41	0.997	2.77	2.22	16.20	0.9990
50	3.80	1.047	0.29	0.996	3.90	0.60	8.69	0.9999
80	6.50	1.250	0.34	0.982	6.40	0.16	7.03	0.9984
100	8.10	0.397	0.14	0.995	7.94	0.19	12.80	0.9996

Table 5
Intra-particle diffusion parameters for the adsorption of Cr(VI) at pH 2.

Concentration (mg L^{-1})	Kid (mg g^{-1} min$^{-1/2}$)	I (mg g^{-1})	r^2
10	0.3075	0.2078	0.9612
40	0.2018	2.1865	0.9728
50	0.3471	2.7456	0.9590
80	1.0256	3.0084	0.8842
100	0.7486	5.1853	0.9894

3.8. Breakthrough capacity

Break through curve is the most effective column process making the optimum use of the concentration gradient between the solute adsorbed by the adsorbent and that remaining in the solution. The column is operational until the metal ions in the effluent start appearing and for practical purposes the working life of the column is over called breakthrough point. This is important in process design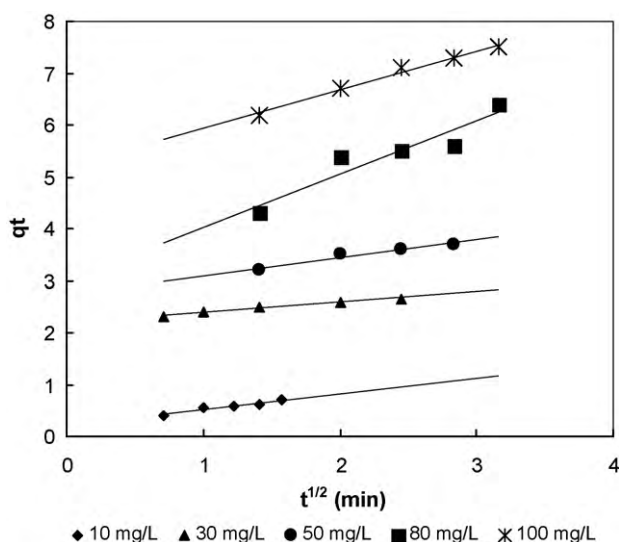 because it directly affects the feasibility and eco-nomics of the process [48]. Fig. 8 shows breakthrough curve when a solution containing 50 mg L^{-1} Cr(VI) passed through the column packed with 0.5 g adsorbent at pH 2. The curve indicates that 50 mL of Cr(VI) solution can be passed through the column without detecting Cr(VI) in the effluent. The breakthrough capacity and exhaustive capacities were found to be 5 and 23.1 mg g^{-1} respectively.

3.9. Treatment of electroplating wastewater

The analysis of electroplating wastewater is reported in Table 6. On comparing the analysis of electroplating wastewater before and after treatment it can be inferred that electroplating wastewater can be treated more efficiently by column process as concentration of Cr(VI) reduced from 58 to 7 mg L^{-1} corresponding to 87.93% removal of Cr(VI).
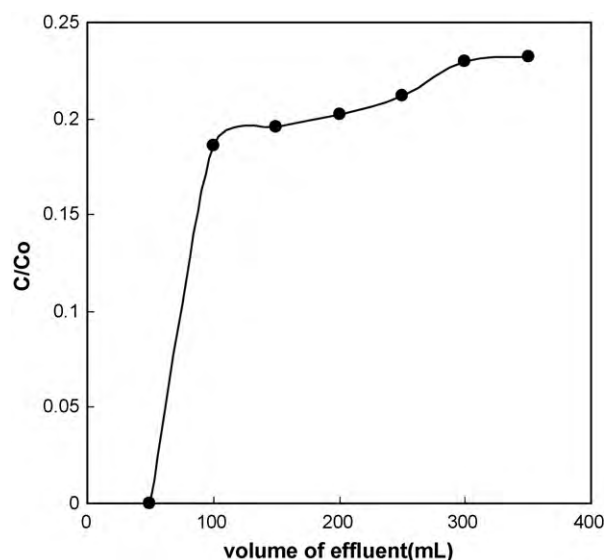

Fig. 7. Intra-particle diffusion.

Fig. 8. Breakthrough capacity.

Table 6
Analysis of electroplating wastewater.

Parameters	Concentration (mg L^{-1})
pH	5.60
TDS	700.00
Na$^+$	160.00
K$^+$	2.00
Ca^{2+}	29.00
Cu^{2+}	5.60
Cd^{2+}	1.30
Zn^{2+}	0.99
Ni^{2+}	2.00
Cr^{6+}	58.00

Table 7
Comparison of the adsorption capacities for Cr(VI) onto various adsorbents.

Adsorbent	Adsorption capacity (mg g^{-1})	Reference
Spirogyra sp.	14.70	[49]
Coconut shell based activated carbon	20.00	[50]
Palm pressed-fibers	15.00	[51]
Almond	10.00	[52]
Distillery sludge	5.70	[53]
Walnut shell	1.33	[54]
Soya cake	0.28	[54]
Ficus glomerata	46.73	Present study

The maximum adsorption capacity of Ficus for Cr(VI) is compared with other adsorbents, reported in the literature are listed in Table 7. The adsorption capacity of Ficus is comparable or higher than those reported earlier.

4. Conclusions

Removal of Cr(VI) from water and electroplating wastewater has been carried out using *F. glomerata* as low-cost adsorbent. The adsorption properties have been explored using batch process. The results can be summarized as follows.

(1) Adsorption of Cr(VI) increases with increase in initial concentration and is strongly affected by pH. The maximum adsorption occurs at pH 2.
(2) The effect of electrolyte (KNO$_3$) on Cr(VI) adsorption is not significant at pH 2.
(3) Thermodynamic parameters indicate adsorption is endothermic and spontaneous. The mean free energy value describes that adsorption is chemical in nature.
(4) Langmuir isotherm model is better obeyed at 50 °C as indicated by chi-square test.
(5) Kinetic data show that pseudo-second order rate equation is followed by the system since q_e values calculated from the model are very close to q_e determined experimentally.
(6) The adsorbent used for the removal of Cr(VI) along with other ions like Cu(II), Ni(II) and Zn(II) from electroplating wastewater shows that 74 and 87% Cr(VI) can be removed using batch and column processes respectively.
(7) The adsorbent can be utilized to reduce the Cr(VI) concentration from 58 to 7 mg L^{-1} in the treatment of electroplating wastewater.

References

[1] R.S. Prakasham, J.S. Merrie, R. Sheela, N. Saswathi, S.V. Ramakrisha, Biosorption of chromium (VI) by free and immobilized Rhizopus arrizus, Environ. Pollut. 104 (1999) 421–427.
[2] S.M. Nomanbhay, K. Palanisamy, Removal of heavy metal from industrial wastewater using chitosan coated oil palm shell charcoal, Electon. J. Biotecnol. 8 (1) (2005) 43–53.
[3] C. Raji, T.S. Anirudhan, Batch Cr(VI) removal by polyacrylamide-grafted sawdust: kinetics and thermodynamics, Water Res. 32 (1998) 3772–3780.
[4] F.C. Richard, A.C.M. Bourg, Aqueous geochemistry of chromium: a review, Water Res. 25 (27) (1991) 807–816.
[5] WHO, Guidelines for Drinking Water Quality, vol. 1, 2nd ed., World Health Organization, 1993.
[6] D. Mohan, K.P. Singh, V.K. Singh, Removal of hexavalent chromium from aqueous solution using low cost activated carbons derived from agricultural waste materials and activated carbon fabric cloth, Ind. Eng. Chem. Res. 44 (4) (2005) 1027–1042.
[7] G. Tiravanti, D. Ptruzzelli, R. Passino, Pretreatment of tannery waste waters by an ion-exchange process for Cr(III) removal and recovery, Water Sci. Technol. 36 (2–3) (1997) 197–207.
[8] C.A. Kozlowski, W. Walkwiak, Removal of chromium (VI) from aqueous solution by polymer inclusion membranes, Water Res. 36 (2002) 4870–4876.
[9] N. Kongsricharoern, C. Poolprasert, Chromium removal by a bipolar electrochemical precipitation process, Water Sci. Technol. 34 (1996) 109–116.
[10] J.J. Testa, M.A. Grela, M.I. Litter, Heterogeneous photo-catalytic reduction of chromium(III) over TiO$_2$ particle in the presence of oxalate: involvement of chromium(VI) species, Environ. Sci. Technol. 38 (5) (2002) 1589–1594.
[11] V.K. Gupta, A.K. Shrivastava, N. Jain, Biosorption of chromium(VI) from aqueous solution by green algae spirogyra species, Water Res. 35 (2001) 4079–4085.
[12] M. Yavuz, F. Gode, E. Pehlivan, S. Ozmert, Y.C. Sharma, An economic removal of Cu^{2+} and Cr^{3+} on the new adsorbents: Pumice and polyacrylonitrile/pumice composite, J. Chem. Eng. 137 (2008) 453–461.
[13] P. Goyal, S. Shrivastava, Characterization of novel Zea mays based biomaterial designed for toxic metals biosorption, J. Hazard. Mater. 172 (2009) 1206–1211.
[14] Y.S. Sharma, B. Singh, A. Agrawal, C.H. Weng, Removal of chromium by Riverbed sand: effect of important parameters, J. Hazard. Mater 15 (2008) 789–793.
[15] P. Sharma, P. Kumari, M.M. Srivastava, S. Srivastava, Ternary biosorption studies of Cd(II) and Cr(III) and Ni(II) on shelled Moringa olifera seeds, Bioresour. Technol. 98 (2) (2007) 474–477.
[16] P. Goyal, P. Sharma, S. Shrivastava, M.M. Shrivastava, Potential of *Saraca indica* leaf powder (SLIP) for chromium removal from aqueous solution, Arch. Environ. Prot. 33 (2007) 35–44.
[17] O.D. Uluozlu, A. Sari, M. Tuzen, M. Soylak, Biosorption of Pb(II) and Cr(III) from aqueous solution by lichen (*Parmelina tiliaceae*) biomass, Bioresour. Technol. (2008) 2972–2980.
[18] J.R. Memon, S.Q. Memon, M.I. Bhanger, A. El-Turki, K.R. Hallam, G.C. Allen, Banana peel: a green and economical sorbent for the selective removal of Cr(VI) from industrial wastewater, Colloids Surf. B 66 (2009) 232–237.
[19] J. Acharya, J.N. Sahu, B.K. Sahoo, C.R. Mohanty, B.C. Meikap, Removal of chromium(VI) from aqueous solution by activated carbon developed from *Tamarind wood* activated with zinc chloride, J. Chem. Eng. 150 (2009) 25–39.
[20] A. El Nemr, Potential of pomegranate husk cabon for Cr(VI) removal from wastewater: kinetic and isotherm studies, J. Hazard. Mater. 161 (2009) 132–141.
[21] M. Jain, V.K. Garg, K. Kadirvelu, Chromium(VI) removal from aqueous system using *Haliantus annuus*(sunflower stems) stem waste, J. Hazard. Mater. 162 (2009) 365–372.
[22] H. Gao, Y. Liu, G. Zeng, W. Xu, T. Li, W. Xia, Characterization of Cr(VI) removal from aqueous solutions by a surplus agricultural waste—rice straw, J. Hazard. Mater. 150 (2008) 446–452.
[23] P. Goyal, S. Shrivastava, Role of biosorbent *Ficus relegiosa* leaf powder (FRLP) in chemical speciation of chromium: a green method for separation, Arch. Environ. Prot. 34 (2008) 35–45.
[24] C.-H. Weng, Y.C. Sharma, S.-H. Chu, Adsorption of Cr(VI) from aqueous solution by spent activated clay, J. Hazard. Mater. 155 (2008) 65–75.
[25] C.V. Rao, A.R. Verma, M.V. Kumar, S. Rastogi, Gastro-protective effect of standardized extract of *Ficus glomerata* fruit on experimental gastric ulcers in rats, J. Ethnophamacol. 115 (2) (2008) 323–326.
[26] D.H. Lataye, I.M. Mishra, I.D. Mall, Removal of pyridine from aqueous solution by adsorption on bagasse fly ash, Ind. Eng. Chem. Res. 45 (2006) 3934–3943.
[27] R. Chand, K. Narimura, H. Kawakita, K. Ohto, T. Watari, K. Inoue, Grape waste as a biosorbent for removing Cr(VI) from aqueous solution, J. Hazard. Mater. 163 (2009) 245–250.
[28] M. Iqbal, A. Saeed, S.I. Zafar, FTIR spectroscopy, kinetics and adsorption isotherm modeling, ion exchange and EXD analysis of understanding the mechanism of Cd^{2+} and Pb^{2+} removal by mango peel waste, J. Hazard. Mater. 164 (2009) 161–171.
[29] Ghodbana, Q. Hamdaoui, Removal of mercury (II) from aqueous media using eucalyptus bark: kinetic and equilibrium studies, J. Hazard. Mater. 160 (2008) 301–309.
[30] S.A. Dean, J.M. Tobin, Uptake of chromium cations and anions by milled peat, Resour. Conserv. Recycl. 27 (1999) 151–156.
[31] R.S. Prakasham, J.S. Merrie, R. Sheela, N. Saswathi, S.V. Ramakrisha, Biosorption of chromium(VI) by free and immobilized *Rhizopus arrhizus*, Environ. Pollut. 104 (1999) 421–427.

[32] Y. Saga, T. Kutsal, Application of adsorption isotherms to chromium adsorption on *Z.ramigera*, Biotechnol. Lett. 11 (1989) 141–144.

[33] X.-P. Liao, W. Tang, R.-Q. Zhou, B. Shi, Adsorption of metal anions of vanadium(V) and chromium(VI) on Zr(IV)-impregnated collagen fiber, Adsorption 14 (2008) 55–64.

[34] A. Baran, E. Bicak, S.H. Baysal, S. Onal, Comparative studies on the adsorption of Cr(VI) ions onto various sorbents, Bioresour. Technol. 98 (2007) 661–665.

[35] H. Ucun, Y.K. Bayhan, Y. Kaya, A. Cakici, O.F. Algm, Biosoption of Cr(VI) from aqueous solution by cone biomass of *Pinus Sylvestris*, Bioresour. Technol. 85 (2002) 155–158.

[36] B.M. Babic, S.K. MLonjie, M.J. Polovina, B.V. Kaludierovic, Point of zero charge and intrinsic equilibrium constants of activated carbon cloth, Carbon 37 (1999) 477–481.

[37] M. Ajmal, R.A.K. Rao, R. Ahmad, J. Ahmad, Adsorption studies on *Citrus reticulates* (fruit peel of orange): removal and recovery of Ni(II) from electroplating waste water, J. Hazard. Mater. B 87 (2001) 127–137.

[38] Y.S. Ho, Selection of optimum sorption isotherm, Carbon 42 (2004) 2113–2130.

[39] L. Ghodbane, O. Nouri, M. Hamdaoui, Chiha, Kinetic and equilibrium study for sorption of Cd(II) ions from aqueous phase by Eucalyptus bark, J. Hazard. Mater. 152 (2008) 148–158.

[40] M.M. Dubinin, L.V. Radushkevich, Proc. Acad. Sci. USSR, Phys. Chem. Sect. 55 (1947) 331.

[41] F. Helfferich, Ion-exchange, Mc Graw Hill, New York, 1962.

[42] C. Namasivayam, K. Ranganatham, Removal of Cd(II) from waste water by adsorption on waste Fe (III)/Cr (III) hydroxides, Water Res. 29 (1995) 1737–1744.

[43] D.J.O. Shannessy, D.J. Winzor, Interpretation of deviation from pseudo-first-order kinetics behavior in the characterization of ligand binding by biosensor technology, Anal. Biochem. 236 (2) (1996) 275–283.

[44] Y.S. Ho, G. Mckay, The kinetics of sorption of divalent ions onto sphagnum moss peat, Water. Res. 34 (2000) 735–742.

[45] Y.S. Ho, C.C. Wang, Pseudo-isotherm for the adsorption of cadmium ion onto tree fern, Process. Biochem. 39 (6) (2004) 761–765.

[46] W.J. Weber Jr., J.C. Morris, Kinetics of adsorption on carbon from solution, J. Sanitary Eng. Div. 89 (1963) 31–59.

[47] B. Volesky, Sorption and Biosorption, BV. Sorbex Inc., Montreal, Canada, 2003, pp.183–185.

[48] V.K. Gupta, A.K. Shrivastava, N. Jain, Biosorptin of chromium(VI) from aqueous solutions by green algae *Spirogyra* species, Water Res. 35 (2001) 4079–4085.

[49] G.J. Alaerts, V. Jitjaturant, P. Kelderman, Use of coconut shell based activated carbon for chromium(VI) removal, Water Sci. Technol. 21 (1989) 1701–1704.

[50] W.T. Tan, S.T. Ooi, C.K. Lee, removal of chromium (VI) from solution by coconut husk and palm pressed fibers, Environ. Technol. 14 (1993) 227–282.

[51] M. Dakiky, M. Khamis, A. Manassra, M. Mer'eb, Selective adsorption of chromium(VI) in industrial wastewater using low-cost abundantly available adsorbents, Adv. Environ. Res. 6 (2002) 533–540.

[52] K. Selvaraj, S. Manonmani, S. Pattabhi, Removal of hexavalent chromium using distillery sludge, Bioresour. Technol. 89 (2003) 207–211.

[53] Y. Orhan, H. Buyukgungur, The removal of heavy metals by using agricultural wastes, Water Sci. Technol. 28 (1993) 247–255.

[54] N. Deneshver, D. Salari, S. Aber, Chromium adsorption and Cr(VI) reduction to trivalent chromium in aqueous solutions by soya cake, J. Hazard. Mater. B 94 (2002) 49–61.